Analysis of Time Response of Lossy Multiconductor Transmission Line Networks

ANTONIJE R. DJORDJEVIĆ AND TAPAN K. SARKAR, SENIOR MEMBER, IEEE

Abstract—**Systems are considered consisting of an arbitrary number of multiconductor transmission lines joined and terminated by arbitrary linear networks. The lines are assumed to be lossy, with frequency-dependent parameters. The system is analyzed in the frequency domain, and the inverse Fourier transform is used to obtain the time-domain response.**

I. INTRODUCTION

MULTICONDUCTOR transmission lines are frequently encountered in digital computers, communication systems, and power distribution systems. Quite often, systems are formed of such lines, which are mutually interconnected (e.g., digital computer buses with branchings). Due to the interconnections and to improper line terminations, the signals propagating in such systems can suffer multiple reflections, which might cause problems, especially in digital circuits. In addition, the dispersive propagation along the lines, which is caused by line losses as well as by the inhomogeneous dielectric in which the lines are embedded, introduces signal distortions and cross talk between the line conductors.

Although the analysis of such systems seems to be of great practical importance, especially in the design of fast digital circuits, there seem to be no references in the open literature treating this problem comprehensively. The present paper is aimed at partly filling this gap.

In this paper a method is developed for analyzing the time-domain response of systems consisting of an arbitrary number of multiconductor transmission lines which are mutually interconnected and terminated by arbitrary linear networks. The lines can be lossy and they can have frequency-dependent parameters. The system can be excited by an arbitrary number of generators, which are located in the terminal and interconnecting networks. An example of such a system is sketched in Fig. 1. The time-domain waveforms of the generators are first Fourier transformed. Next, the analysis of the system is performed in the frequency domain at a set of discrete frequencies. Finally, the inverse fast Fourier transform is used to obtain the time-domain waveforms.

The transmission line analysis is based on the modal theory in the frequency domain, which can be found in many references, e.g. [1]. Each of the lines is assumed to be uniform along its length, and it is described in terms of the circuit-theory parameters. At each frequency, the line eigenmodes are evaluated and they are combined with the equations describing the terminal and interconnecting networks to obtain the response of the whole system. The basic relations for multiconductor transmission lines which are relevant to the present analysis are summarized in Section II.

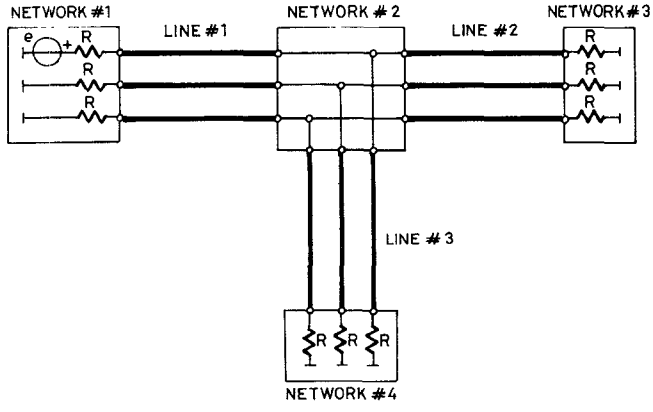

Fig. 1. Sketch of a system with three multiconductor transmission lines.

The transmission lines are assumed to be mutually interconnected and terminated in an arbitrary manner by linear multiport networks. These networks can, for example, contain equivalent excess capacitances and inductances describing line junctions and ends. Generators exciting the system can be included in any of the interconnecting and terminal networks. The terminal and interconnecting networks can conveniently be described in the frequency domain by two square matrices and a column matrix (vector), as shown in Section III.

The equations describing the transmission lines and those describing the terminal and interconnecting networks form a system of simultaneous linear equations. This system can be solved in the frequency domain to obtain the voltages at the transmission line ends. By applying the inverse Fourier transform, the voltages in the time domain are obtained, which represent the final solution. The combined treatment of the transmission lines and of the terminal and interconnecting networks is described in Section IV.

In Section V, some numerical examples are shown to illustrate the application of the present technique. The

Manuscript received February 9, 1987; revised June 8, 1987. This work was supported in part by E. I. du Pont de Nemours & Co.

A. R. Djordjević is with the Department of Electrical Engineering, University of Belgrade, P.O. Box 816, 11001 Belgrade, Yugoslavia.

T. K. Sarkar is with the Department of Electrical and Computer Engineering, Syracuse University, Syracuse, NY 13244-1240.

IEEE Log Number 8716526.

0018-9480/87/1000-0898$01.00 ©1987 IEEE

examples include single multiconductor transmission lines, cascaded lines, branchings, and loops formed by transmission lines.

II. Treatment of Multiconductor Transmission Lines

In this section we are going to briefly summarize the main equations which are necessary to analyze lossy multiconductor transmission lines, starting from the line circuit-theory parameters. The derivation of these equations can be found, for example, in [1].

Let us consider only one transmission line at a time (Fig. 2). Let it have N signal conductors, and a ground (reference) conductor. (We assume that the ground is at a zero potential for all multiconductor transmission lines of our system.) The transmission line is assumed to be of an arbitrary cross section, which is uniform along the line length.

Let us introduce a local x axis along the length of our transmission line, with $x = 0$ corresponding to the first end of the line and $x = D$ corresponding to the second end of the line. We assume that we know the following line parameters: the matrix $[L]$ of inductances per unit length, the matrix $[R]$ of resistances per unit length, the matrix $[B]$ of electrostatic induction coefficients per unit length, and the matrix $[G]$ of conductances per unit length. All these matrices are of dimensions $N \times N$. (We are not going to discuss the evaluation of these quasi-TEM matrices, and the reader can refer, for example, to [2]–[5] for numerical methods for the computation of the matrices $[L]$, $[B]$, $[R]$, and $[G]$.) The line can be described by the telegrapher equations in the frequency domain:

$$\frac{d[V(x)]}{dx} = -[Z'][I(x)] \tag{1}$$

$$\frac{d[I(x)]}{dx} = -[Y'][V(x)] \tag{2}$$

where $[V(x)]$ is the vector of complex line voltages, $[I(x)]$ is the vector of complex line currents,

$$[Z'] = [R] + j\omega[L] \tag{3}$$

$$[Y'] = [G] + j\omega[B] \tag{4}$$

and ω is the angular frequency. From the telegrapher equations, the wave equation for the line voltage vector can be derived:

$$\frac{d^2[V(x)]}{dx^2} = [Z'][Y'][V(x)], \qquad 0 < x < D. \tag{5}$$

Next, we try to find a solution to the wave equation (5) which is a wave whose propagation along the line is described by the multiplicative factor $\exp(\pm \gamma_m x)$, i.e.,

$$[V^m(x)] = [V_0^m]\exp(\pm \gamma_m x) \tag{6}$$

$$[I^m(x)] = [I_0^m]\exp(\pm \gamma_m x) \tag{7}$$

where $[V_0^m]$ and $[I_0^m]$ are vectors of complex constants. Such waves are referred to as the eigenmodes. The minus sign in (7) corresponds to a mode traveling in the direction of the x axis (the incident wave), and the plus sign corresponds to a mode traveling in the opposite direction (the reflected wave).

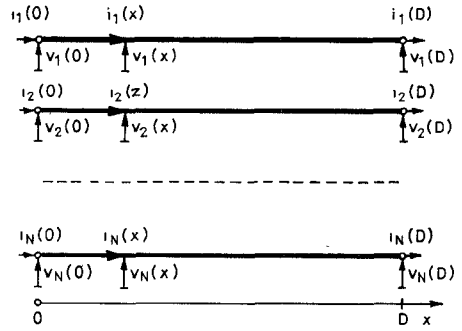

Fig. 2. Sketch of a multiconductor transmission line.

From the wave equation (5), we now obtain

$$\{\gamma_m^2[U] - [Z'][Y']\}[V_0^m] = 0 \tag{8}$$

where $[U]$ is an identity matrix. Equation (8) has nontrivial solutions for the vector $[V_0^m]$ if

$$\det\{\gamma_m^2[U] - [Z'][Y']\} = 0. \tag{9}$$

The solutions to (9) are N complex numbers γ_m^2 $(m = 1, \cdots, N)$, which are referred to as the eigenvalues. Each eigenvalue has its corresponding eigenvector $[V_0^m]$, which is a solution to (8) and is unique to a multiplicative constant. By taking square roots of the eigenvalues, the modal propagation coefficients γ_m are evaluated.

Next, we define the modal voltage matrix $[S_V]$, the columns of which are the vectors $[V_0^m]$, and the modal current matrix $[S_I]$, the columns of which are the vectors $[I_0^m]$ $(m = 1, \cdots, N)$. These modal matrices are related as

$$[S_I] = [Z']^{-1}[S_V][\Gamma] \tag{10}$$

where

$$[\Gamma] = \text{diag}\{\gamma_1, \cdots, \gamma_N\}. \tag{11}$$

In the general case, all the eigenmodes, propagating in both directions, will be excited on the transmission line. Let us introduce complex intensities of the incident and reflected modes at $x = 0$, G_{i0}^m and G_{r0}^m $(m = 1, \cdots, N)$. Then the voltages of the mth eigenmode at $x = 0$ are given as $(G_{i0}^m + G_{r0}^m)[V_0^m]$, while the currents can be obtained as $(G_{i0}^m - G_{r0}^m)[I_0^m]$, where the vectors $[V_0^m]$ and $[I_0^m]$ correspond to incident waves.

Transmission line voltages and currents at any position x along the line can be written as sums of the incident and reflected waves:

$$[V(x)] = [V_i(x) + V_r(x)] = [S_V]\{[G_i(x)] + [G_r(x)]\} \tag{12}$$

$$[I(x)] = [I_i(x) - I_r(x)] = [S_I]\{[G_i(x)] - [G_r(x)]\} \tag{13}$$

where

$$[G_i(x)] = [E(x)][G_{i0}] \tag{14}$$

$$[G_r(x)] = [E(x)]^{-1}[G_{r0}]. \tag{15}$$

$[G_{i0}]$ and $[G_{r0}]$ are complex vectors containing modal intensities at $x=0$, and

$$[E(x)] = \operatorname{diag}(\exp(-\gamma_1 x), \cdots, \exp(-\gamma_N x)). \quad (16)$$

The characteristic impedance matrix $[Z_c]$ of the line is defined by the relations

$$[V_i(x)] = [Z_c][I_i(x)] \qquad [V_r(x)] = -[Z_c][I_r(x)] \quad (17)$$

and it can be evaluated as

$$[Z_c] = [S_V][S_I]^{-1} = [S_V][\Gamma]^{-1}[S_V]^{-1}[Z']. \quad (18)$$

The inverse of $[Z_c]$ is the characteristic admittance matrix $[Y_c]$.

If we introduce $[E_D] = [E(D)]$ and $[G_{rD}] = [E_D]^{-1}[G_{r0}]$, we obtain voltages and currents at both transmission line ends in terms of the incident modal intensities at $x=0$ and the reflected modal intensities at $x=D$:

$$[V(0)] = [S_V]([G_{i0}] + [E_D][G_{rD}]) \quad (19)$$

$$[I(0)] = [Y_c][S_V]([G_{i0}] - [E_D][G_{rD}]) \quad (20)$$

$$[V(D)] = [S_V]([E_D][G_{i0}] + [G_{rD}]) \quad (21)$$

$$[I(0)] = [Y_c][S_V]([E_D][G_{i0}] - [G_{rD}]). \quad (22)$$

Note that the reference directions for the line currents coincide with the direction of the x axis (as shown in Fig. 2).

From the above equations, it can be seen that the state at the transmission line ends is uniquely determined by $2N$ quantities, i.e., by the elements of the modal intensity vectors $[G_{i0}]$ and $[G_{rD}]$. The objective of our analysis will be to find these vectors for each transmission line (at a set of discrete frequencies) by a combined treatment of the transmission lines and the terminal and interconnecting networks.

III. Treatment of Terminal and Interconnecting Networks

We assume that the networks terminating and interconnecting the transmission lines of our system are arbitrary multiport linear networks, some of which contain generators. Also, we assume that there are no dependent generators in one network which depend on the state in another network; i.e., we assume that these networks are coupled only through the transmission lines. (If there is another coupling between two networks, we simply combine the two networks into one network.)

One or more transmission lines are connected to each terminal or interconnecting network. We impose no restrictions on the way the transmission lines are connected, except that each end of a line is entirely connected to one network. One transmission line can be connected at both ends to the same network, two or more lines can link two networks, the lines can form loops, etc. The transmission lines can be terminated in an arbitrary manner. For example, a line conductor can be short-circuited to the ground,

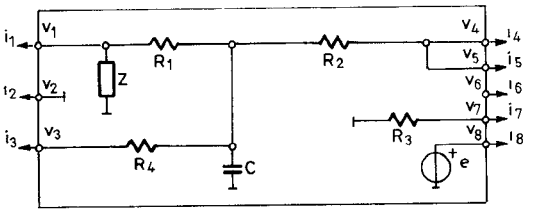

Fig. 3. Sketch of an interconnecting network.

it can be left opened, it can be terminated in an arbitrary impedance, it can be driven by a generator, or it can be connected to a conductor belonging to the same or to another transmission line.

Nodes of a terminal or interconnecting network can be divided into two groups. The first group comprises the nodes at which the transmission lines are connected. These nodes we shall refer to as the external nodes. The second group comprises all the other nodes, which we shall refer to as the internal nodes. We assume that the networks have the same common ground as the transmission lines. The number of external nodes for a network must be equal to the total number of signal conductors of all the transmission lines connected to that network. Let this number be M. Let us introduce the vector $[V]$ of voltages between the network external nodes and ground, and the vector $[I]$ of currents leaving the network through the external nodes (Fig. 3). The network being linear, there exists a matrix relation between these two vectors which has the general form

$$[P][V] + [Q][I] = [E] \quad (23)$$

where $[P]$ and $[Q]$ are square matrices of dimensions $M \times M$, and $[E]$ is a column matrix of dimensions $M \times 1$. Equation (23) includes both Z-parameter and Y-parameter representations of the network. In the case of the Z-parameter representation, we have $[P] = [U]$, $[Q] = [Z]$, and $[E] = [V_0]$, where $[U]$ is an identity matrix, $[Z]$ is the matrix of the Z parameters, and $[V_0]$ is the vector of the open-circuit voltages. This is, essentially, Thévenin's equivalent representation of the network. In the case of the Y-parameter representation, we have $[P] = [Y]$, $[Q] = [U]$, and $[E] = [I_0]$, where $[Y]$ is the matrix of the Y parameters, and $[I_0]$ is the vector of the short-circuit currents. This is Norton's equivalent representation. However, in the general case, the elements of the matrices $[P]$, $[Q]$, and $[E]$ need not be of the same kind, and we have a hybrid representation of the network.

The general equation (23) for the terminal and interconnecting networks can easily describe any kind of a network, unlike the Z parameters and Y parameters. Namely, the Z parameters cannot be defined in the presence of open circuits, while the Y parameters cannot be defined for short circuits.

For networks which contain no internal nodes, (23) can easily be obtained by writing down the nodal equations. In these equations, the currents leaving the network through the external nodes have to be included, and the nodal voltages coincide with the elements of the vector $[V]$. For

networks which do not have internal loops (i.e., closed paths along the branches which completely lie within the network), (23) can be obtained from the mesh equations, in which the voltages between the external nodes and the ground are involved. In that case, the mesh currents coincide (within a sign) with the elements of the vector $[I]$.

Some examples of the matrices $[P]$, $[Q]$, and $[E]$ are given in Section V.

IV. Combined Treatment of Transmission Lines and Terminal and Interconnecting Networks

Once we know the equivalent representation of the terminal and interconnecting networks, we have to combine these equations with the equations describing the transmission lines. In order to facilitate the work, it is convenient to order the M external nodes of each network so that the first N_1 nodes belong to the transmission line #1 connected to that network, the next N_2 nodes belong to the line #2 connected to that network, etc. Note that the network voltages coincide with the corresponding voltages of the transmission line. However, the network currents are equal to the transmission line currents only if the network is connected to the first end of the line. If the network is connected to the second end of the line, then the network currents are the negative of the corresponding transmission line currents. This is due to the adopted reference directions for current, as shown in Figs. 2 and 3.

Our objective in this paper is to solve for the voltages at the transmission line ends. To that purpose, we can replace the first N_1 elements of the network voltage vector $[V]$ with the corresponding elements of the voltage vector of the first transmission line connected to the network, then replace the following N_2 elements with the corresponding elements of the voltage vector for the second line, etc. Then, we repeat the same procedure for the network current vector $[I]$, substituting for its elements the corresponding elements of the current matrices of the transmission lines, taking into account a possible change of the sign. In other words, we replace blocks of the network vectors $[V]$ and $[I]$ with the appropriate transmission line vectors $[V]$ and $[I]$. Next, we substitute transmission line voltages and currents from (19)–(22) in terms of the line modal intensities $[G_{i0}]$ and $[G_{rD}]$. Finally, we plug the network vectors $[V]$ and $[I]$ into (23). This equation now represents M linear equations relating the modal intensities of the lines connected to the network.

If we write such equations for all the terminal and interconnecting networks, we actually obtain a definite system of linear equations in $[G_{i0}]$ and $[G_{rD}]$ for all the lines. The number of unknowns in this system equals twice the total number of conductors of all the lines. Equivalently, it equals the total number of external nodes for all the terminal and interconnecting networks.

If we solve this system, we obtain the line modal intensities $[G_{i0}]$ and $[G_{rD}]$. These intensities known, we can easily compute the voltages at the line ends, from (19) and (21), which was precisely our objective. Also, we can evaluate the currents at the line ends, from (20) and (22), or voltages and currents at any cross section along any line.

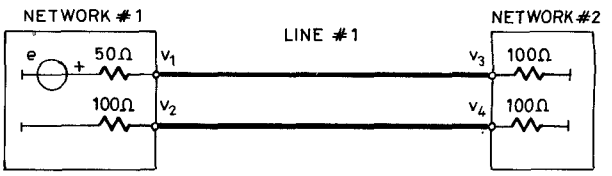

Fig. 4. Sketch of a transmission line with terminal networks.

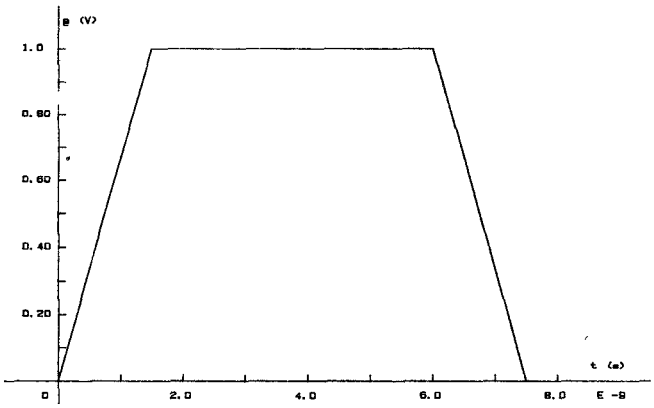

Fig. 5. Generator electromotive force.

A particular problem can arise if the frequency is zero. If the lines are lossless, or at least one of the lines matrices $[R]$ or $[G]$ is zero, the eigenvalue equation (9) has no solution, because the product $[Z'][Y'] = [0]$. Although special equations for the system could be constructed in such a case, this would be extremely complicated because many transmission lines can be present in the system, and the terminal and interconnecting networks can have elements whose immittances become singular at the zero frequency (e.g., capacitors and inductors). In order to avoid this problem, instead of analyzing the system at a zero frequency, we can analyze the system at a very low frequency, and treat the results as if they were for the zero frequency. Since we utilize the fast Fourier transform to relate the time-domain data to the frequency-domain data, we involve only discrete frequencies. In that case, a "very low frequency" could be, for example, 1/100 of the distance between adjacent samples in the frequency domain.

V. Numerical Examples

As the first example, we consider a single multiconductor transmission line, with $N = 2$. One line conductor is driven by a 50-Ω generator at one end, while all the other line ports are connected to the ground by 100-Ω resistors. The system is sketched in Fig. 4. Note that in Fig. 4 the ground conductor is not shown, in order to simplify the scheme. We first assume the line to be lossless and 0.3048 m long and the line parameters to be

$$[L] = \begin{bmatrix} 494.6 & 63.3 \\ 63.3 & 494.6 \end{bmatrix} \text{nH/m}$$

$$[B] = \begin{bmatrix} 62.8 & -4.9 \\ -4.9 & 62.8 \end{bmatrix} \text{pF/m}.$$

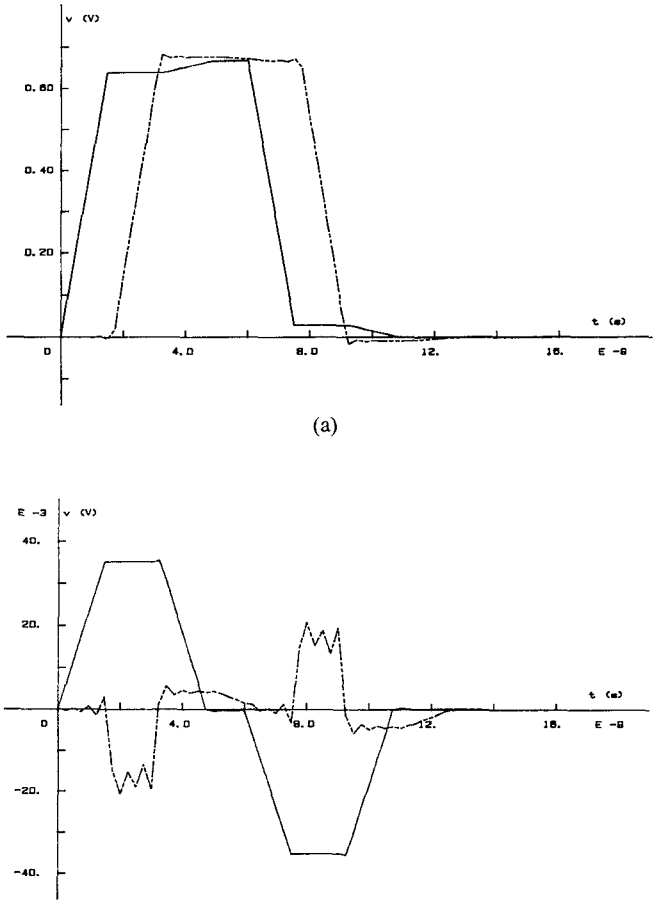

Fig. 6. Voltages for the system of Fig. 4 (lossless case): (a) —— v_1 and ---- v_3; (b) —— v_2 and ---- v_4.

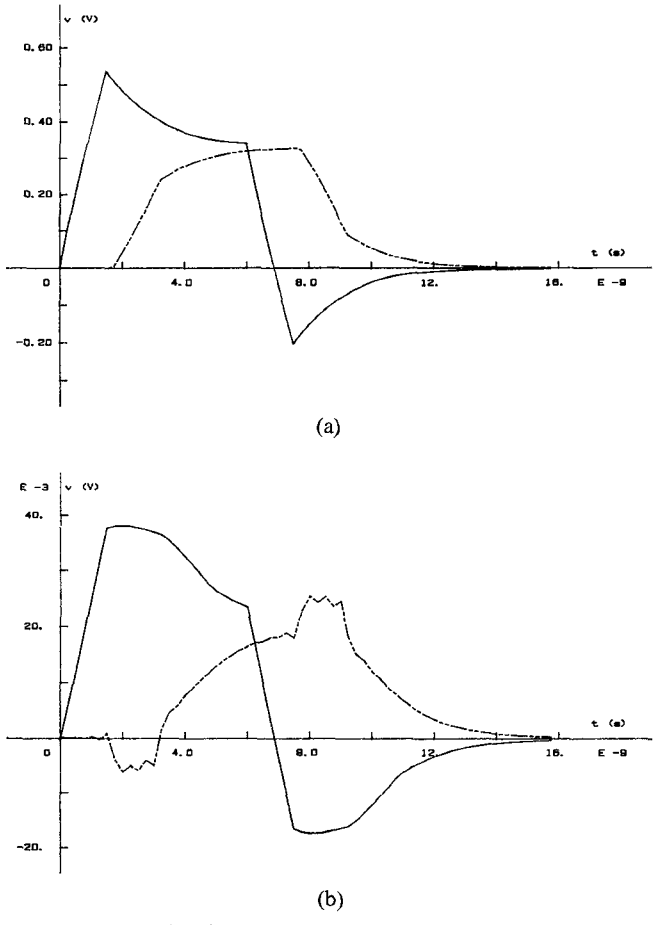

Fig. 7. Voltages for the system of Fig. 4 (lossy case): (a) —— v_1 and ---- v_3; (b) —— v_2 and ---- v_4.

The electromotive force of the generator driving the line is shown in Fig. 5. The same emf is also used in all the other examples in this paper.

In this case there are two terminal networks and only one line. If we take a Z-parameter representation of the terminal networks, we obtain the following matrices describing the terminal networks:

$$[P_1]=\begin{bmatrix}1 & 0\\ 0 & 1\end{bmatrix} \quad [Q_1]=\begin{bmatrix}50 & 0\\ 0 & 100\end{bmatrix}\Omega \quad [E_1]=\begin{bmatrix}E(f)\\ 0\end{bmatrix}$$

$$[P_2]=\begin{bmatrix}1 & 0\\ 0 & 1\end{bmatrix} \quad [Q_2]=\begin{bmatrix}100 & 0\\ 0 & 100\end{bmatrix}\Omega \quad [E_2]=\begin{bmatrix}0\\ 0\end{bmatrix}$$

where $E(f)$ is the Fourier transform of the emf shown in Fig. 5. The voltages at the line ends, obtained by the present method, are shown in Fig. 6. As in all the other examples presented below, the time interval for the fast Fourier transform was taken to be $\Delta t = 0.25$ ns. The number of samples in the time domain for this example was 64. (All the examples presented in this paper were run on a Digital Professional 350 personal computer.) The ripple in the plotted results, which is particularly visible in the voltage at the second end of the parasitic line, is caused by a relatively small number of samples used in the analysis.

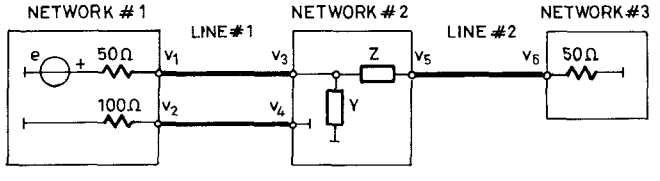

Fig. 8. Sketch of two cascaded transmission lines.

Next, we consider the same case as shown in Fig. 4, but we assume the line to be lossy. The line resistance matrix is assumed to vary in proportion to the square root of the frequency, while the conductance matrix is assumed to be independent of the frequency. The resistance matrix at 1 MHz and the conductance matrix are given by

$$[R]=\begin{bmatrix}0.1 & 0.02\\ 0.02 & 0.1\end{bmatrix}\Omega/\text{m}$$

$$[G]=\begin{bmatrix}0.1 & -0.01\\ -0.01 & 0.1\end{bmatrix}\text{S/m}.$$

The resulting voltage waveforms are shown in Fig. 7.

As the second system, we consider the two transmission lines sketched in Fig. 8, one having two signal conductors, and the other one signal conductor. Both lines are assumed to be lossless. The matrices $[L]$ and $[B]$ for the first line are the same as for the previous example. (The diagonal elements of the characteristic impedance matrix are 89 Ω,

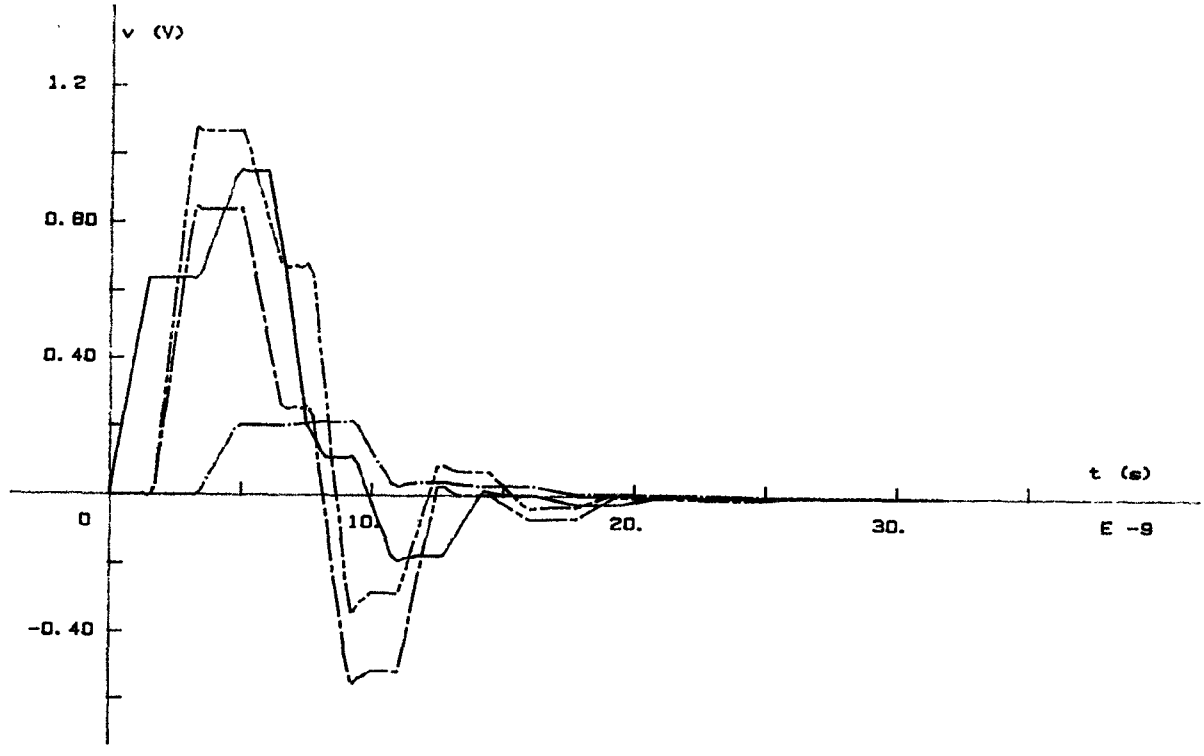

(a)

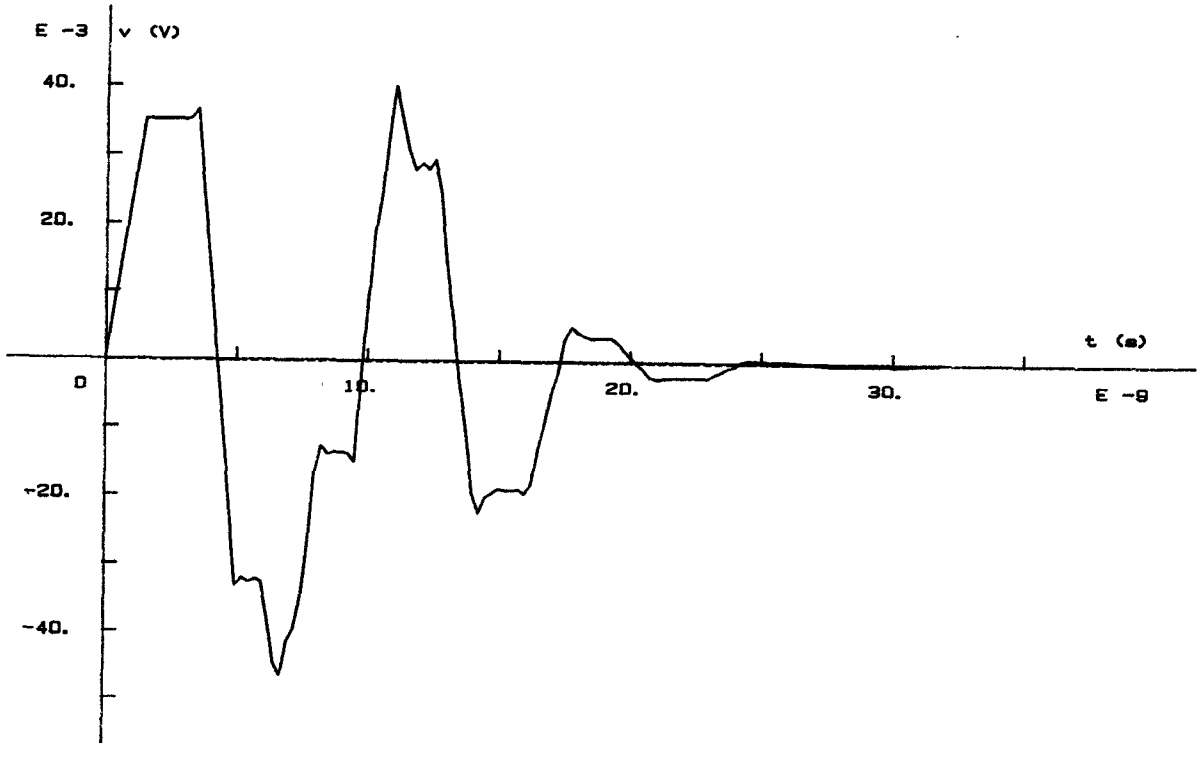

(b)

Fig. 9. Voltages for the system of Fig. 8 (with a 100-Ω series resistor at the junction): (a) —— v_1, ---- v_3, –– –– v_5, and —·— v_6; (b) —— v_2.

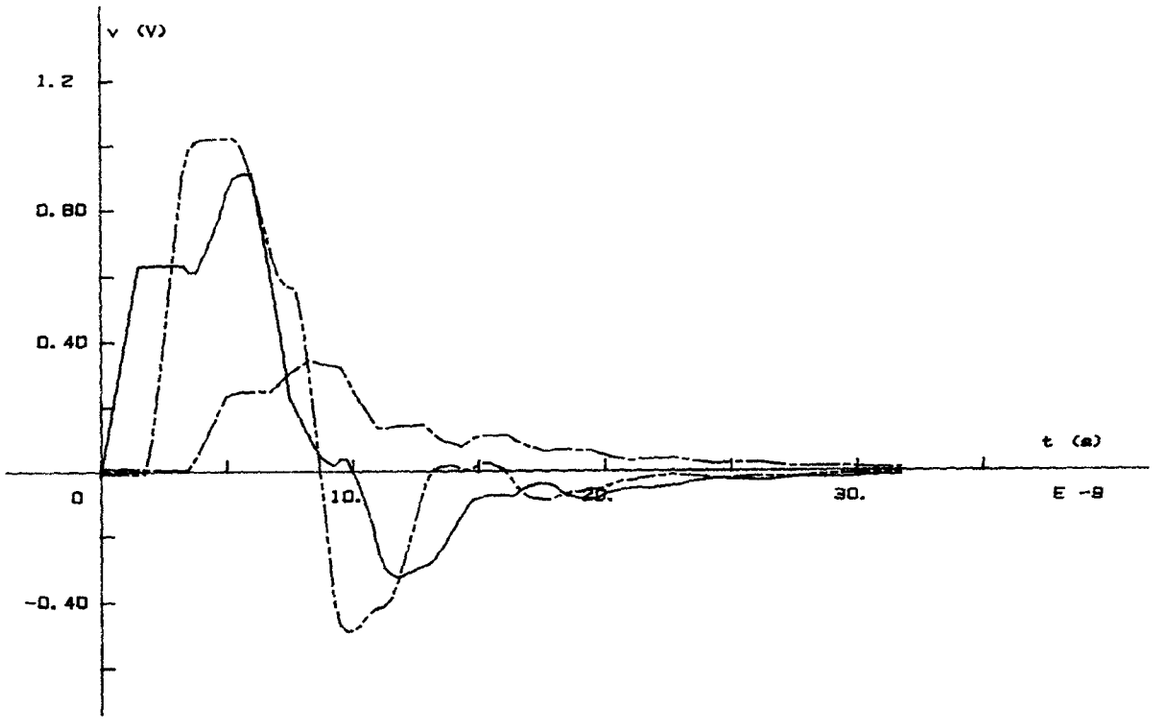

(a)

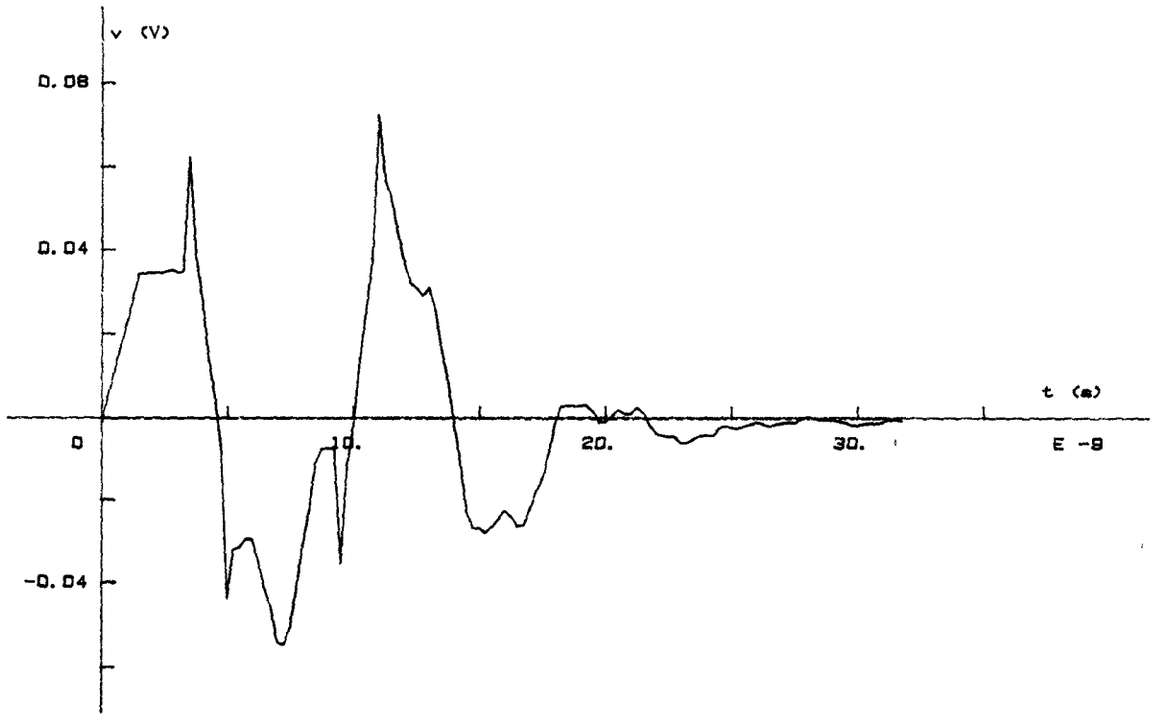

(b)

Fig. 10. Voltages for the system of Fig. 8 (with a 3.18-pF parallel capacitor at the junction): (a) —— v_1, ---- v_3, and —·— v_6; (b) —— v_2.

and the off-diagonal elements are 9.2 Ω.) For the second line, it was assumed that $L = 2$ μH/m and $B = 15$ pF/m (i.e., the characteristic impedance of the line is 365 Ω). Both lines are of the same length, 0.3048 m. The matrices describing the interconnecting network are

$$[P_2] = \begin{bmatrix} 1 & -1 & 0 \\ 0 & 0 & 1 \\ Y & 0 & 0 \end{bmatrix} \quad [Q_2] = \begin{bmatrix} 0 & -Z & 0 \\ 0 & 0 & 0 \\ 1 & 0 & 1 \end{bmatrix}$$

$$[E_2] = \begin{bmatrix} 0 \\ 0 \\ 0 \end{bmatrix}.$$

The matrices describing the first terminal network are the same as for the system of Fig. 4, while for the second terminal network we have

$$[P_3] = [1] \quad [Q_3] = [50]\ \Omega \quad [E_3] = [0].$$

First, it was assumed that $Z = 100$ Ω and $Y = 0$, i.e., that there is a 100-Ω resistor connected between the driven conductor of the first line and the second line. The resulting voltages are shown in Fig. 9, where it is easy to see how the excited wave propagates down the first line, how it gets reflected at the interconnection with the second line due to a high mismatch (the characteristic impedance of the second line being about four times greater than the diagonal element of the characteristic impedance matrix of the first line), and how the mismatch at the end of the second line affects the voltage at the interconnection between the two lines.

In the second case, a capacitance was assumed to be connected in parallel with the junction between the two lines, i.e., $Z = 0$ and $Y = j\omega C$, with $C = 3.18$ pF. (This capacitance could represent the excess capacitance of the junction.) The resulting waveforms are shown in Fig. 10. The waveforms at the driven conductor are rounded due to the integrating effect of the capacitor.

The third system considered consists of the three transmission lines, of unequal lengths, sketched in Fig. 11. The first line length is 0.3048 m, the second is 0.4572 m, and the third is 0.6096 m. This system can represent a cable or bus branching. All three lines are lossless and they have the same characteristics as the line of Fig. 4. The matrices describing the first terminal network are the same as before; for network #2 we have

$$[P_2] = \begin{bmatrix} 1 & 0 & -1 & 0 & 0 & 0 \\ 1 & 0 & 0 & 0 & -1 & 0 \\ 0 & 1 & 0 & -1 & 0 & 0 \\ 0 & 1 & 0 & 0 & 0 & -1 \\ 0 & 0 & 0 & 0 & 0 & 0 \\ 0 & 0 & 0 & 0 & 0 & 0 \end{bmatrix}$$

$$[Q_2] = \begin{bmatrix} 0 & 0 & 0 & 0 & 0 & 0 \\ 0 & 0 & 0 & 0 & 0 & 0 \\ 0 & 0 & 0 & 0 & 0 & 0 \\ 0 & 0 & 0 & 0 & 0 & 0 \\ 1 & 0 & 1 & 0 & 1 & 0 \\ 0 & 1 & 0 & 1 & 0 & 1 \end{bmatrix} \quad [E_2] = \begin{bmatrix} 0 \\ 0 \\ 0 \\ 0 \\ 0 \\ 0 \end{bmatrix}$$

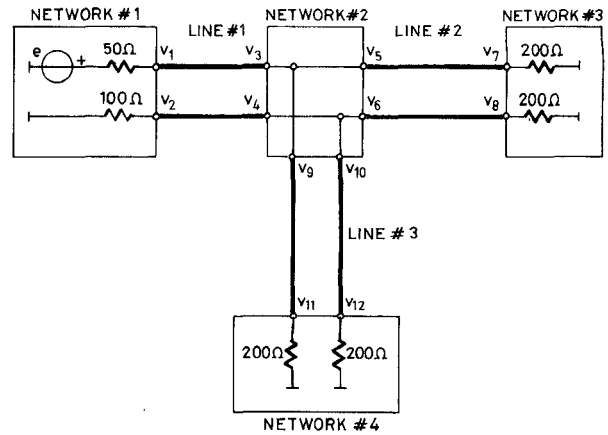

Fig. 11. Sketch of a transmission line branching.

while for networks #3 and #4 we have

$$[P_3] = [P_4] = \begin{bmatrix} 1 & 0 \\ 0 & 1 \end{bmatrix} \quad [Q_3] = [Q_4] = \begin{bmatrix} 200 & 0 \\ 0 & 200 \end{bmatrix} \Omega$$

$$[E_3] = [E_4] = \begin{bmatrix} 0 \\ 0 \end{bmatrix}.$$

The voltage waveforms for this system are shown in Fig. 12. In this figure one can see that the second and third lines initially represent a mismatch to the first line (as if the first line were terminated in one half of its characteristic impedance matrix). Ultimately, however, it becomes well matched, because of the 200-Ω resistors, which, for a late time, can be considered to be connected in parallel. Note that a T junction of three conductors cannot be made well matched at more than one port (unless the junction is a resistive network), which might cause problems in any kind of line branching.

The final example is a three-line system, shown in Fig. 13. The two lines with two signal conductors have the same characteristics as the line of Fig. 4, while the line with one signal conductor has $L = 494.6$ nH/m and $B = 62.8$ pF/m. All three lines are of the same length, 0.3048 m. Again, the first network is the same as the one in Fig. 5, while for the other two networks we have

$$[P_2] = \begin{bmatrix} 1 & 0 & -1 & 0 & 0 \\ 1 & 0 & 0 & 0 & -1 \\ 0 & 1 & 0 & -1 & 0 \\ 0 & 0 & 0 & 0 & 0 \\ 0 & 0 & 0 & 0 & 0 \end{bmatrix}$$

$$[Q_2] = \begin{bmatrix} 0 & 0 & 0 & 0 & 0 \\ 0 & 0 & 0 & 0 & 0 \\ 0 & 0 & 0 & 0 & 0 \\ 1 & 0 & 1 & 0 & 1 \\ 0 & 1 & 0 & 1 & 0 \end{bmatrix} \quad [E_2] = \begin{bmatrix} 0 \\ 0 \\ 0 \\ 0 \\ 0 \end{bmatrix}$$

$$[P_3] = \begin{bmatrix} 1 & 0 & 0 \\ 0 & 1 & -1 \\ 0 & 0 & 0 \end{bmatrix} \quad [Q_3] = \begin{bmatrix} 100\Omega & 0 & 0 \\ 0 & 0 & 0 \\ 1 & 0 & 1 \end{bmatrix}$$

$$[E_3] = \begin{bmatrix} 0 \\ 0 \\ 0 \end{bmatrix}.$$

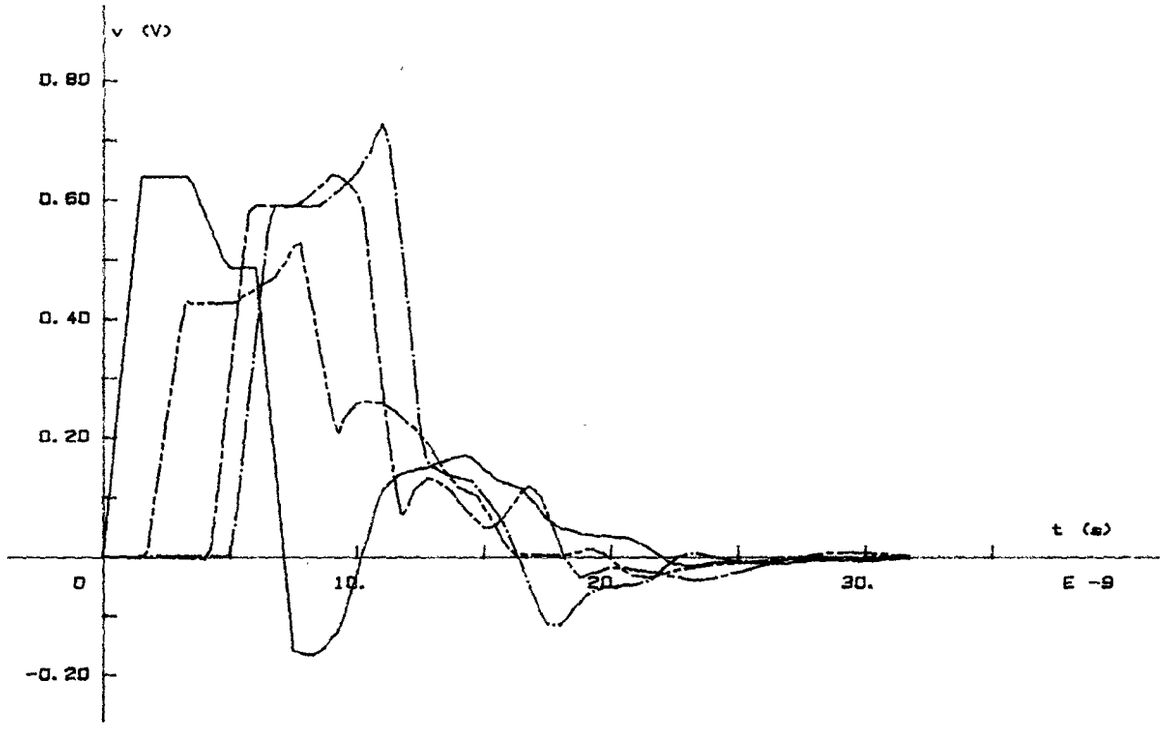

(a)

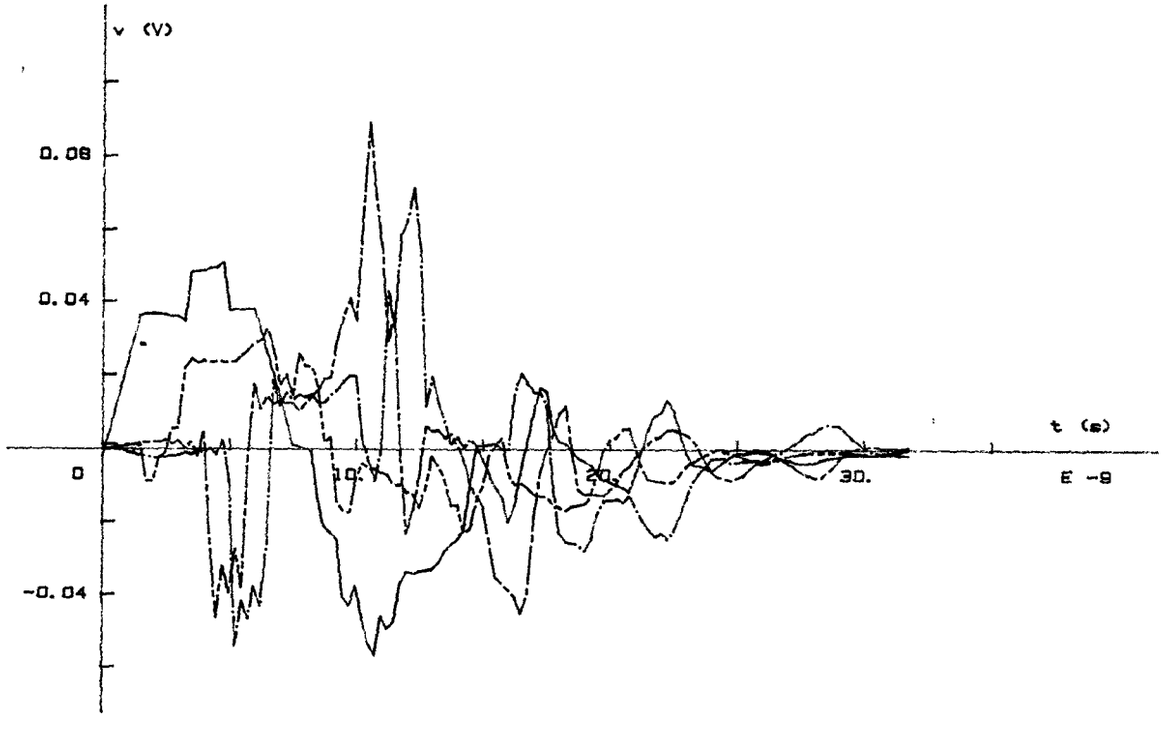

(b)

Fig. 12. Voltages for the system of Fig. 11: (a) —— v_1, ---- v_3, —— v_7, and —·— v_{11}; (b) —— v_2, ---- v_4, —— v_8, and —·— v_{12}.

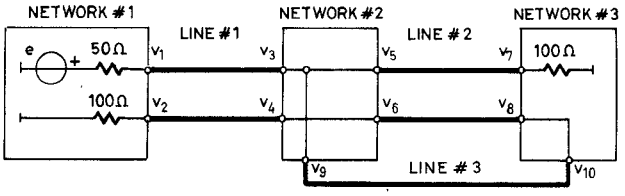

Fig. 13. Sketch of a transmission line loop.

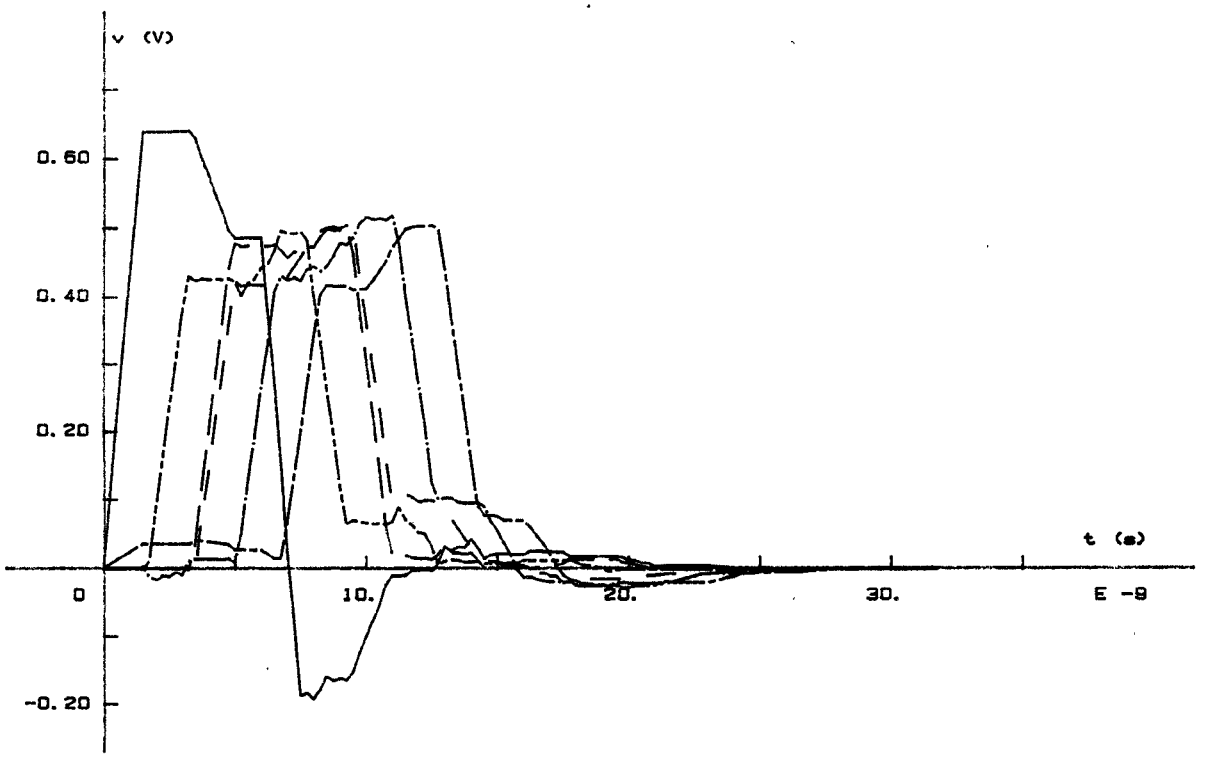

Fig. 14. Voltages for the system of Fig. 13: —— v_1, —·— v_2, ——— v_3, —·— v_4, — — v_7, and – – v_8.

The voltages at the transmission line ends are plotted in Fig. 14. The wave first propagates down the first line (the dominant voltage is at the driven conductor); then it gets separated along the upper conductor of the second line and along the third line. The voltages along these two paths are almost the same (except for a small influence of the lower conductor of the second line), and they arrive almost coincidently to the third network. The voltage at the upper conductor of the second line practically does not get reflected, because it sees a well-matched termination, while the third line excites the lower conductor of the second line. This excited wave travels back along the second line and excites the lower conductor of the first line. Again, this wave sees a reasonably good termination at the first network, so that the system response dies out pretty fast.

VI. Conclusions

A computer-oriented technique for evaluating the time-domain response of a system consisting of a number of arbitrarily interconnected lossy multiconductor transmission lines was presented. The technique can be applied even on personal computers to obtain waveforms propagated along systems with line branchings and loops, which can be of particular value in the design of printed-circuit interconnections of fast digital computers. A few examples were presented illustrating this technique and demonstrating wave reflections, distortions, and cross talk.

References

[1] S. Frankel, *Multiconductor Transmission Line Analysis*. Norwood, MA: Artech House, 1977.

[2] C. Wei, R. F. Harrington, J. R. Mautz, and T. K. Sarkar, "Multiconductor transmission lines in multilayered dielectric media," *IEEE Trans. Microwave Theory Tech.*, vol. MTT-32, pp. 439–450, Apr. 1984.

[3] R. F. Harrington and C. Wei, "Losses on multiconductor transmission lines in multilayered dielectric media," *IEEE Trans. Microwave Theory Tech.*, vol. MTT-32, pp. 705–710, July 1984.

[4] J. Venkataraman, S. M. Rao, A. R. Djordjević, T. K. Sarkar, and Y. Naiheng, "Analysis of arbitrarily oriented microstrip transmission lines in arbitrarily shaped dielectric media over a finite ground plane," *IEEE Trans. Microwave Theory Tech.*, vol. MTT-33, pp. 952–959, Oct. 1985.

[5] A. R. Djordjević, T. K. Sarkar, and S. M. Rao, "Analysis of finite conductivity cylindrical conductors excited by axially independent TM electromagnetic field," *IEEE Trans Microwave Theory Tech.*, vol. MTT-33, pp. 960–966, Oct. 1985.

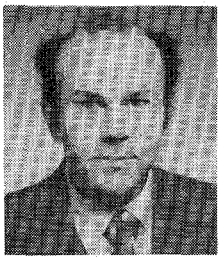

Antonije R. Djordjević was born in Belgrade, Yugoslavia, in 1952. He received the B.Sc., M.Sc., and D.Sc. degrees from the University of Belgrade in 1975, 1977, and 1979, respectively.

In 1975, he joined the Department of Electrical Engineering, University of Belgrade, as a Teaching Assistant in Electromagnetics. In 1982, he was appointed Assistant Professor of Microwaves in the same department. From February 1983 until February 1984, he was with the Department of Electrical Engineering, Rochester Institute of Technology, Rochester, NY, as a Visiting Associate Professor. His research interests are numerical problems in electromagnetics, especially those applied to antennas and microwave passive components.

✠

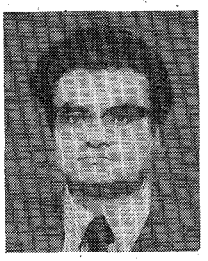

Tapan K. Sarkar (S'69–M'76–SM'81) was born in Calcutta, India, on August 2, 1948. He received the B. Tech. degree from the Indian Institute of Technology, Kharagpur, in 1969, the M.Sc.E. degree from the University of New Brunswick, Fredericton, N.B., Canada, in 1971, and the M.S. and Ph.D. degrees from Syracuse University, Syracuse, NY, in 1975.

From 1969 to 1971, he served as an Instructor at the University of New Brunswick. While studying at Syracuse University, he served as an Instructor and Research Assistant in the Department of Electrical and Computer Engineering. From 1976 to 1985, he was with the Rochester Institute of Technology. In 1977 and 1978, he was a Research Fellow at the Gordon McKay Laboratory at Harvard University. Currently, he is associated with Syracuse University. His research interests deal with the numerical solution of operator equations arising in electromagnetics and signal processing.

Dr. Sarkar is an associate editor of the IEEE TRANSACTIONS ON ELECTROMAGNETIC COMPATIBILITY, an associate editor for feature articles in the IEEE TRANSACTIONS ON ANTENNAS AND PROPAGATION NEWSLETTER, and is on the editorial board of *Journal of Electromagnetic Waves and Applications*. He is also the Vice-Chairman of the URSI International Commission on Time Domain Metrology. Dr. Sarkar is a professional engineer registered with the state of New York and a member of Sigma Xi and URSI Commission A and B.